



The relevance of T2 relaxation time in interpreting MRI apparent diffusion coefficient (ADC) map for musculoskeletal structures

Yi Xiang J. Wáng¹, Maria Pilar Aparisi Gómez^{2,3,4}, Fernando Ruiz Santiago^{5,6}, Alberto Bazzocchi⁷

¹Department of Imaging and Interventional Radiology, Faculty of Medicine, The Chinese University of Hong Kong, Hong Kong SAR, China; ²Department of Radiology, Auckland District Health Board, Auckland, New Zealand; ³Department of Anatomy and Medical Imaging, Faculty of Medical and Health Sciences, The University of Auckland, Auckland, New Zealand; ⁴Department of Radiology, IMSKE, Valencia, Spain; ⁵Department of Radiology and Physical Medicine, Faculty of Medicine, University of Granada, Granada, Spain; ⁶Musculoskeletal Radiology Unit, Hospital Universitario Virgen de Las Nieves, Granada, Spain; ⁷Diagnostic and Interventional Radiology, IRCCS Istituto Ortopedico Rizzoli, Bologna, Italy

Correspondence to: Yi Xiang J. Wáng, MMed, PhD. Department of Imaging and Interventional Radiology, Faculty of Medicine, The Chinese University of Hong Kong, 30-32 Ngan Shing Street, Shatin, New Territories, Hong Kong SAR, China. Email: yixiang_wang@cuhk.edu.hk

Keywords: Magnetic resonance imaging (MRI); apparent diffusion coefficient (ADC); T2 relaxation time; musculoskeletal

Submitted Oct 04, 2023. Accepted for publication Oct 17, 2023. Published online Oct 20, 2023.

doi: 10.21037/qims-23-1392

View this article at: <https://dx.doi.org/10.21037/qims-23-1392>

Random movement (“molecular diffusion”) of particles comes from the thermal energy that they possess at any given temperature above absolute zero. A self-diffusion coefficient of around $2.3 \times 10^{-3} \text{ mm}^2/\text{s}$ has been demonstrated earlier by a sample that contains small molecules, for example, water, at approximately 25 °C (room temperature) (1). This motion of water molecules can be hampered by the presence of cell membranes and macromolecules, and the *in vivo* organ apparent diffusion coefficients (ADCs) measured by magnetic resonance imaging (MRI) are expected to be smaller than *in vitro* water phantom value. On the other hand, *in vivo* organ ADC is also contributed by tissue perfusion. In body water, such as the case of gallbladder, ADC is measured to be around $3 \times 10^{-3} \text{ mm}^2/\text{s}$ (2), which is affected by the body temperature, composition of bile fluid, as well as the body bulk motion due to respiration and cardiovascular pulsating, etc.

ADC values of some *in vitro* phantom results, *in vivo* muscle, cartilage, intervertebral disc NP and IAF (nucleus pulposus and inner annulus fibrosus) (3), and bone marrow are listed in *Table 1* (4–20). Liver, the largest solid organ in the body, has an ADC of around $1.07 \times 10^{-3} \text{ mm}^2/\text{s}$ (6), and also considering free water has an *in vitro* ADC of around $2.2 \times 10^{-3} \text{ mm}^2/\text{s}$ (4,6), we intuitively feel that the ADCs of

cartilage (around $1.5 \times 10^{-3} \text{ mm}^2/\text{s}$) and disc NP and IAF (around $1.9 \times 10^{-3} \text{ mm}^2/\text{s}$) are ‘unrealistically high’. Compared with the liver ADC of $1.07 \times 10^{-3} \text{ mm}^2/\text{s}$ and spleen ADC of $0.8 \times 10^{-3} \text{ mm}^2/\text{s}$ (6), muscle ADC, being around $1.55 \times 10^{-3} \text{ mm}^2/\text{s}$, also appears to be high. Recently, Wáng *et al.* (21–25) proposed that *in vivo* ADC measure is strongly associated with T2 relaxation time (T2 time) [*Table 2, Figure 1* (26–44)]. Wáng *et al.* (24) divide T2 time into short T2 time band (<60 ms), intermediate T2 time band (60–80 ms), and long T2 time band (>80 ms, all 3 T values). For the short T2 time band, there is a negative correlation between T2 time and ADC. For the long T2 time band, there is a positive correlation between T2 time and ADC. A tissue likely measures a low ADC if its T2 time is close to 70 ms. The phenomenon shown in *Figure 1* can help explain the counterintuitive ADC values commonly seen in a number of musculoskeletal tissues.

In experimental studies, it was suggested that the hepatic blood volume including that of the large vessels is about 25 mL/100 g, whereas this value is 3 mL/100 g in skeletal muscle (45). Though we would think that the ADC of muscles will not be higher than that of liver with the liver more richly perfused by hepatic artery and portal vein and with lots of sinusoids and space of Disse, however, muscles

Table 1 A list of ADC values of some phantoms, muscle, cartilage, intervertebral disc NP and IAF, and bone marrow

Authors	Materials/tissues	Mean ADC ($\times 10^{-3}$ mm ² /s)	Magnet [#]	b value (s/mm ²) ^{§§}
Kalaitzakis <i>et al.</i> (4)	Water phantom	2.20	1.5 T	0–1,500, 10 b values
Kalaitzakis <i>et al.</i> (4)	5% sucrose solution phantom	1.88	1.5 T	0–1,500, 10 b values
Gatidis <i>et al.</i> (5)	Water phantom	2.15	3.0 T	0–1,000, 10 b values
Gatidis <i>et al.</i> (5)	Polyethylene glycol (10 mM) phantom	1.86	3.0 T	0–1,000, 10 b values
Kim <i>et al.</i> (6)	Liver ^{##}	1.07	3.0 T	0, 800
Kim <i>et al.</i> (6)	Spleen	0.79	3.0 T	0, 800
Sandberg <i>et al.</i> (7)	Muscles (11.2 years) [¶]	1.48	3.0 T	50, 600
Chen <i>et al.</i> (8)	Paraspinal muscle (57.0 years) [¶]	1.55	3.0 T	50, 800
Padhani <i>et al.</i> (9)	Psoas muscle [¶]	1.39	1.5 T	50, 800 (or 900)
Raya <i>et al.</i> (10)	Muscle (review) [¶]	1.60	3.0 T	
Zbýň <i>et al.</i> (11)	Knee articular cartilage	1.90	3.0 T	50, 500, 100
Ukai <i>et al.</i> (12)	Knee articular cartilage (51.5 years)	1.40	3.0 T	0, 600
Raya <i>et al.</i> (10)	Articular cartilage (review)	1.50	3.0 T	
Hamaguchi <i>et al.</i> (13)	Disc NP and IAF (33.4 years) ^{¶¶}	1.78	3.0 T	0, 1,000
Shen <i>et al.</i> (14)	Disc NP and IAF (24.3 years) ^{¶¶}	1.99	1.5 T	0, 800
Niu <i>et al.</i> (15)	Non-degenerated NP and IAF (20–29 years)	2.16	1.5 T	0, 500
Niinimäki <i>et al.</i> (16)	Non-degenerated NP (49 years)	1.65	1.5 T	0, 500
Sandberg <i>et al.</i> (7)	Red bone marrow (11.2 years) [§]	0.86	3.0 T	50, 600
Padhani <i>et al.</i> (9)	Red bone marrow [§]	0.68	3.0 T	50, 800 (or 900)
Zbýň <i>et al.</i> (11)	Bone marrow (knee) [§]	0.53	3.0T	50, 500, 100
Padhani <i>et al.</i> (9)	Yellow bone marrow [§]	0.38	1.5 T	50, 800 (or 900)
Byun <i>et al.</i> (17)	Sacrum yellow bone marrow (70 years) [§]	0.21	1.5 T	0, 650
Raya <i>et al.</i> (10)	Bone marrow (review) [§]	0.45	3.0 T	–

[#], it is generally considered that diffusion is *per se* not a nuclear magnetic resonance phenomenon. Magnetic field strength should have little impact on ADC values measured (18,19); ^{##}, older age is commonly associated with higher liver iron content and higher fat content, both can lead to lower ADC measure (20); [¶], muscle fascia contain fat. In a defined muscle region, fat portion in the fascia may increase in older subjects, and this leads to lower muscle ADC measure; ^{¶¶}, discs of mixed degeneration grading; [§], bone marrow ADC depends on the ratio of red marrow to yellow marrow. The data of Sandberg *et al.* (7) may be closer to pure red marrow ADC; ^{§§}, ADC measure is affected by b value selection during data acquisition and the noise levels, however, besides muscle, perfusion contribution to ADC is small for most of the skeletal tissues. ADC, apparent diffusion coefficient; NP, nucleus pulposus; IAF, inner annulus fibrosus.

have a shorter T2 time than the liver (*Table 2*). In the study of Wall *et al.* (26), muscle measured an ADC of 29 ms whereas liver measured an ADC of 45 ms at 0.35 T. In the study of de Bazelaire *et al.* (27), muscle measured an ADC of 29 ms whereas liver measured an ADC of 46 ms at 1.5 T. The phenomenon as demonstrated in *Figure 1* shows, with liver data as the reference, the shorter T2 time of muscles is associated with an increased ADC value for the muscle

(relative to the liver). *Figure 1* also helps to explain that cartilage and disc NP and IAF measure very high ADC not because these tissues have true high tissue diffusivity, but instead because of their T2 times being both away from the intermediate T2 time band of 60–80 ms (at 3 T). Moreover, cartilage and disc NP and IAF demonstrate high ADC due to the opposite reasons, with cartilage having a relatively short T2 time and non-degenerated disc NP and IAF

Table 2 A list of T2 time values of some musculoskeletal structure and disorders and tumors of the body and brain

Authors	Tissues	Mean T2 (ms)	Magnet [#] (T)
Wall <i>et al.</i> (26)	Liver	45	0.35
de Bazelaire <i>et al.</i> (27)	Liver (31.5 years)	34 [¶]	3.0
de Bazelaire <i>et al.</i> (27)	Liver (31.5 years)	46	1.5
Bogaert <i>et al.</i> (28)	Liver (47.1 years)	46	1.5
Wall <i>et al.</i> (26)	Muscle	29	0.35
de Bazelaire <i>et al.</i> (27)	Paravertebral muscle (31.5 years)	29	3
Lang <i>et al.</i> (29)	Leg muscle in rat	33	2.0
Pettersson <i>et al.</i> (30)	Muscle	32	0.15
Gold <i>et al.</i> (31)	Muscle (27–38 years)	32	3.0
Gold <i>et al.</i> (31)	Muscle (27–38 years)	35	1.5
Raya <i>et al.</i> (10)	Muscle (review)	32	3.0
Gold <i>et al.</i> (31)	Knee articular cartilage (27–38 years)	37	3
Gold <i>et al.</i> (31)	Knee articular cartilage (27–38 years)	42	1.5
Roth <i>et al.</i> (32)	Knee articular cartilage (16 years)	38	3.0
Ukai <i>et al.</i> (12)	Knee articular cartilage (51.5 years)	40	3.0
Ruiz Santiago <i>et al.</i> (33)	Patellar cartilage (16–45 years)	41	1.5
Raya <i>et al.</i> (10)	Articular cartilage (review)	37	3.0
Niu <i>et al.</i> (15)	Non-degenerated discs NP and IAF (20–29 years)	164	1.5
Wang <i>et al.</i> (34)	Non-degenerated discs NP and IAF (32 years)	130	3.0
Yang <i>et al.</i> (35)	Non-degenerated discs NP and IAF (44 years)	138	3.0
Stelzeneder <i>et al.</i> (36)	Non-degenerated discs NP (19 years)	238	3.0
Bouhsina <i>et al.</i> (37)	Non-degenerated discs NP and IAF in dog	249	1.5
Wall <i>et al.</i> (26)	Abscess various body sites	81	0.35
Pettersson <i>et al.</i> (30)	Chondrosarcoma	120	0.15
Pettersson <i>et al.</i> (30)	Malignant fibrous histiocytoma	92	0.15
Pettersson <i>et al.</i> (30)	Osteogenic sarcoma	75	0.15
Lang <i>et al.</i> (29)	Osteogenic sarcoma—rat model	73	2.0
Arita <i>et al.</i> (38)	Active prostate cancer bone metastasis	82	3.0
Jung <i>et al.</i> (39)	Breast cancer	90	3.0
Baohong <i>et al.</i> (40)	Parotid gland cancer	97	3.0
Hepp <i>et al.</i> (41)	Prostate cancer	80	3.0
Gu <i>et al.</i> (42)	Grade II glioma	164	3.0
Gu <i>et al.</i> (42)	High-grade glioma	127	3.0
Oh <i>et al.</i> (43)	Gliomas	160	1.5
Oh <i>et al.</i> (43)	Meningiomas/metastases	125	1.5

Data from tumors of the body and brain represent a few random selections for illustration only. [#], there is a notion that T2 time does not change much over the range of field strengths used for routine clinical MR imaging (0.2 to 3.0 T) (44); [¶], the value of 34 ms for liver at 3.0 T is likely underestimated, i.e., liver T2 time at 3.0 T may be longer. NP, nucleus pulposus; IAF, inner annulus fibrosus; MR, magnetic resonance.

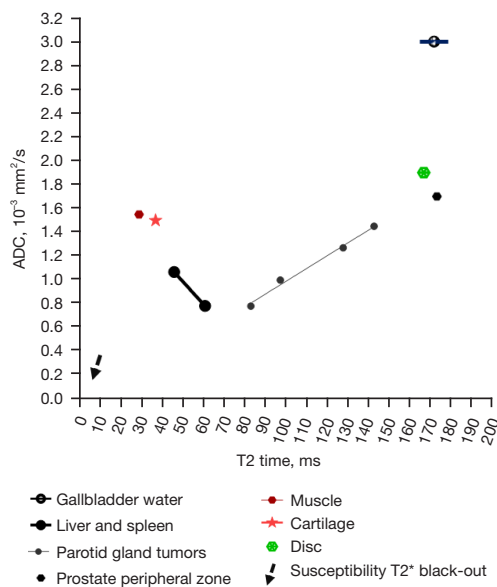


Figure 1 Relationship between T2 time and ADC at 3 T. The graph is initially from Wáng and Ma (24). Data sources for liver, spleen, parotid gland tumors, and prostate also see Wáng and Ma (24). T2 time for the liver is assumed to be 42 ms (Table 2). Data points for muscle, cartilage, and intervertebral disc are newly added (values based on Tables 1,2). There are large variations for reported intervertebral disc T2 time and ADC values, thus mean values for the discs are presented simplistically (the data from dog not counted). For data with T2 time <60 ms, there is a negative correlation between T2 time and ADC. For data with T2 time >80 ms, there is a positive correlation between T2 time and ADC. Dotted arrow denotes susceptibility T2* black-out, which is observed with structures having a very short intrinsic T2 signal due to very short T2*. In this graph, dotted arrow is for illustration only, and does not reflect true quantitative values for susceptibility T2* black-out. ADC, apparent diffusion coefficient.

having a long T2 time (Table 2).

A few musculoskeletal lesions also demonstrate unusual ADC values. Pyogenic abscess fluid (i.e., pus) tends to demonstrate a very low ADC (e.g., $0.63 \times 10^{-3} \text{ mm}^2/\text{s}$) regardless of the location of the abscess (46-49). It is counterintuitive that abscess pus, being fluid or semi-fluid, has a very low ADC measure. Recently Wáng noted that (25), abscess pus having a T2 time of about half that of body water (around 80 ms) contributes to very low ADC measured by MRI [Figure 1, Table 3 (9,17,41,43,48-59)]. Abscess pus may not have truly restricted diffusion compared with many other *in vivo* solid tissues. Morán *et al.* (50) and Einarsdóttir

et al. (51) reported myxoma ADC values of 2.38×10^{-3} and $2.80 \times 10^{-3} \text{ mm}^2/\text{s}$ respectively, which are quite high. Quantitative data on T2 time for musculoskeletal myxoma remain limited, however, it is known that myxoid substance has a long T2 time (as noted with bright signal on T2 weighted images). Myxoma has a high ADC likely due to myxoid substance's long T2 time. Another disease type is chondrosarcoma. Chondrosarcoma has a long T2 time (e.g., 120 ms) and high ADC measure [e.g., $2.3 \times 10^{-3} \text{ mm}^2$, Table 3 (53)]. It is unlikely that chondrosarcoma has a true high tissue diffusivity. T2 shine-through refers to high signal on diffusion weighted images that is not due to restricted diffusion, but rather to long T2 time in some tissue or body fluid (52). It is considered that this T2 shine-through error can be avoided with assessment of the high b value images and the corresponding ADC map. The ADC map is considered to have corrected the T2 shine-through (52). Thus, the ADC measure of lesions such as myxoma cannot be explained by the T2 shine-through effect.

The analyses above further support that T2 time is a dominant contributor to ADC measure (24), and call for re-consideration on whether cellularity or high cell density contributes to tumor ADC. It has been perceived that malignant tissues' ADC is associated with malignant tissues' being generally more cellular than benign tissues and extra-cellular water molecule diffusion in these tissues is lower with anarchic cellular proliferation. While it is possible that a more malignant tumor will deviate more from the native tissue in composition, thus show more deviation in T2 time from native tissue, and thus so does ADC measure, some studies did not report a correlation between ADC measure and cellularity (59-63). For example, Sadeghi *et al.* (60) noted that 'This study, which takes into account the regional heterogeneity of gliomas, does not confirm the inverse correlation between ADC and cell density reported in previous studies. This finding underlines the impact of other determinants of water diffusivity within the complex microenvironment encountered in gliomas. As previously reported, edema, necrosis, and extracellular matrix components constitute some of such parameters that may influence ADC values within gliomas.' The study of Rosenkrantz *et al.* (61) on pancreatic cancer showed no associations between ADCs of pancreatic adenocarcinoma and tumour grade or other adverse pathological features. Nonomura *et al.* (62) reported that there was no ADC difference between normal hematopoietic cell bone marrow without fat infiltration and lymphoma-related hypercellular bone marrow, despite lymphoma tissue had more compacted cells. Table 3 shows

Table 3 A list of ADC values of some musculoskeletal disorders and tumors of the body and brain

Authors	Materials/tissues	Mean ADC ($\times 10^{-3}$ mm ² /s)	Magnet [#]	b value (s/mm ²) ^{§§§}
Subhawong <i>et al.</i> (48)	Abscess in musculoskeletal soft tissue [§]	0.63	3.0 T	50, 400, 800
Erdogan <i>et al.</i> (49)	Abscess in brain	0.69	1.5 T	0, 1,000
Morán <i>et al.</i> (50)	Myxoma	2.38	1.5 T	0,300, 600, 1,000
Einarsdóttir <i>et al.</i> (51)	Myxoma	2.80	1.5 T	0, 600
Subhawong <i>et al.</i> (52)	Myxoid liposarcoma [§]	2.31	Unknown	Unknown
Hayashida <i>et al.</i> (53)	Chondrosarcoma	2.29	1.5 T	0, 500, 1,000
Ahlawat <i>et al.</i> (54)	Enchondroma ^{§§}	1.80	3.0 T	50, 400, 800
Subhawong <i>et al.</i> (48)	Ewings sarcoma [§]	0.80	3.0 T	50, 400, 800
Ahlawat <i>et al.</i> (54)	Osteosarcoma ^{##}	0.80	3.0 T	50, 400, 800
Feuerlein <i>et al.</i> (55)	Soft-tissue tumors (mixed) ^{##}	0.85	1.5 T	0, 150, 500, 1,000
Padhani <i>et al.</i> (9)	Multiple myeloma	0.88	1.5 T	50, 800 (or 900)
Padhani <i>et al.</i> (9)	Breast cancer bone marrow Met	0.94	1.5 T	50, 800 (or 900)
Byun <i>et al.</i> (17)	Sacrum Met (mixed)	0.78	1.5 T	0, 650
Balliu <i>et al.</i> (56)	Vertebral malignancies (mixed)	0.92	1.5 T	0, 500
Feuerlein <i>et al.</i> (55)	Liver malignancies (mixed) ^{##}	0.81	1.5 T	0, 150, 500, 1,000
Feuerlein <i>et al.</i> (55)	Colon/rectum malignancies (mixed) ^{##}	0.92	1.5 T	0, 150, 500, 1,000
Feuerlein <i>et al.</i> (55)	Uterus/ovaries malignancies (mixed) ^{##}	0.77	1.5 T	0, 150, 500, 1,000
Feuerlein <i>et al.</i> (55)	Skeletal Met (mixed) ^{##}	0.81	1.5 T	0, 150, 500, 1,000
Hepp <i>et al.</i> (41)	Prostate cancer	0.76	3.0 T	50, 500, 1,000, 2,000
Surov <i>et al.</i> (57)	Breast cancer liver Met	0.86	1.5 T	0, 600
Thormann <i>et al.</i> (58)	Hepatocellular carcinoma	0.93	1.5 T	0, 500
Oh <i>et al.</i> (43)	Gliomas	1.28	1.5 T	0, 1,000
Oh <i>et al.</i> (43)	Meningiomas/Met	1.10	1.5 T	0, 1,000
Stadnik <i>et al.</i> (59)	Gliomas	1.14	1.5 T	0, 300, 1,200

Data from tumors of the body and brain represent a few random selections for illustration only. [#], it is generally considered that diffusion is *per se* not a nuclear magnetic resonance phenomenon. Magnetic field strength should have little impact on ADC values measured (18,19); [§], result of a single case only; ^{§§}, mineralization leading to lower ADC measures; ^{##}, with limited case number; ^{§§§}, ADC measure is affected by b value selection during data acquisition and the noise levels, however, besides muscle, perfusion contribution to ADC is small for most of the skeletal tissues. ADC, apparent diffusion coefficient; Met, metastasis.

ADCs of myeloma or metastatic malignancies in the bone do not demonstrate major ADC difference with other cancerous tissues such as liver malignancies, colon/rectum malignancies, uterus/ovaries malignancies, and prostate cancer. Brain tumors tend to have a relatively higher T2 time and a relatively higher ADC measure. For most of the tumors originated in the liver or pancreas, with increased T2 time which shifts toward 70 ms, these tumors have a reduced ADC relative to native tissues. For prostate

cancer with a decreased T2 time which shifts toward 70 ms, prostate cancer also has a reduced ADC relative to the native tissue. With T2 time shifting away from 70 ms, brain tumors mostly are associated with increased ADC (24). For soft tissue tumours, Einarsdóttir *et al.* (51) reported ADC values of benign soft tissue tumours and sarcomas overlapped and could not be used to differentiate between the bulk of benign and malignant tumours. Maeda *et al.* (64) also reported that ADCs of benign and malignant soft-tissue

tumors were not significantly different. Balliu *et al.* (56) reported that ADC does not help differentiate spine malignancy from spine infection. Razek *et al.* (65) reported that soft-tissue malignant tumors tend to have a lower mean ADC value than soft-tissue benign tumors. However, there was huge variation among individual cases depending on the histopathological types. An injection of gadolinium contrast agent, which will shorten T2 time of the tissues, has also been reported to be associated with a lower ADC measure (66,67) without the gadolinium contrast agent actually changing the diffusivity of the tissues. For the cases of prostate cancer and breast cancer, gadolinium agent will slightly shift the T2 times of these tissues toward 70 ms. It is also likely that the *in vivo* measurement of ADC is contaminated by bulk motion due to physiological motion (such as respiration and cardiovascular pulsing) and the vibration of MR scanner gradients during diffusion data acquisition. The contribution of cellularity to ADC may be of only minor importance in practice.

Another phenomenon of note is the so-called susceptibility T2* 'black-out', which is seen with structures having a very short intrinsic T2 signal due to very short T2* associated with iron or calcium content (68,69). It is known that hematomas can have a low ADC value. Susceptibility artifacts such as hemorrhage containing deoxyhemoglobin or hemosiderin result in unreliable ADC value calculations with pseudo-low ADC values (68,70,71). Assessing osteosarcoma or osteoblastic bone metastases can also be challenging sometimes due to the presence of this phenomenon (72).

The analyses in this article re-emphasize the notion that, for interpretation of ADC value of any tissue, this tissue's T2 time should be always referred (24). Moreover, some authors reported that ADC does not offer superiority over T2 time in a number of diagnostic analyses. For intracerebral tumors, Oh *et al.* (43) reported T2 values were more useful than ADC for characterizing contrast enhancing tumor and immediate-edema regions of glioma, meningiomas and metastases. Stadnik *et al.* (59) reported that the diffusion-weighted images and ADC maps of gliomas were less useful than the T2-weighted and contrast-enhanced T1-weighted images in definition of tumor boundaries. The ADC values of solid gliomas, metastases, and meningioma were in the same range. In a study of glioma patients, Kinoshita *et al.* (73) reported that ADC was unable to show a significant correlation with ¹¹C-methionine uptake (as shown on positron emission tomography) or with tumor cell density; however, a combination of T1 and T2 relaxation time correlated both with methionine uptake

and tumor cell density. Cieszanowski *et al.* (74) reported significantly higher sensitivity and accuracy of T2 time than ADC for diagnosing hepatic malignancy. ADC maps may suffer from alignment errors between images of different b values and also low signal-to-noise ratio from diffusion-weighted imaging. Within the framework of diffusion weighted imaging, a number of pitfalls have also been noted with intravoxel incoherent (IVIM) analysis (21,75-77). The additional benefits of ADC over T2 time or signal intensity on properly T2 weighted images should be carefully studied further for musculoskeletal application.

Acknowledgments

Funding: None.

Footnote

Conflicts of Interest: The authors have completed the ICMJE uniform disclosure form (available at <https://qims.amegroups.com/article/view/10.21037/qims-23-1392/coif>). YXJW serves as the Editor-in-Chief of *Quantitative Imaging in Medicine and Surgery*. The other authors have no conflicts of interest to declare.

Ethical Statement: The authors are accountable for all aspects of the work in ensuring that questions related to the accuracy or integrity of any part of the work are appropriately investigated and resolved.

Open Access Statement: This is an Open Access article distributed in accordance with the Creative Commons Attribution-NonCommercial-NoDerivs 4.0 International License (CC BY-NC-ND 4.0), which permits the non-commercial replication and distribution of the article with the strict proviso that no changes or edits are made and the original work is properly cited (including links to both the formal publication through the relevant DOI and the license). See: <https://creativecommons.org/licenses/by-nc-nd/4.0/>.

References

1. Mills R. Self-diffusion In Normal and Heavy-water In Range 1-45 Degrees. *J Phys Chem* 1973;77:685-8.
2. Mohajeri S, Ijare OB, Bezabeh T, King SB, Thomas MA, Minuk G, Lipschitz J, Kirkpatrick I, Smith M, Smith IC. In vivo 1H MRS of human gallbladder bile at 3 T in one

- and two dimensions: detection and quantification of major biliary lipids. *NMR Biomed* 2014;27:1192-202.
3. Mok GSP, Zhang D, Chen SZ, Yuan J, Griffith JF, Wang YXJ. Comparison of three approaches for defining nucleus pulposus and annulus fibrosus on sagittal magnetic resonance images of the lumbar spine. *J Orthop Translat* 2016;6:34-41.
 4. Kalaitzakis G, Boursianis T, Gourzoulidis G, Gourtsoyianni S, Lymperopoulou G, Marias K, Karantanas A, Maris TG. Apparent diffusion coefficient measurements on a novel diffusion weighted MRI phantom utilizing EPI and HASTE sequences. *Phys Med* 2020;73:179-89.
 5. Gatidis S, Schmidt H, Martirosian P, Schwenzer NF. Development of an MRI phantom for diffusion-weighted imaging with independent adjustment of apparent diffusion coefficient values and T2 relaxation times. *Magn Reson Med* 2014;72:459-63.
 6. Kim BR, Song JS, Choi EJ, Hwang SB, Hwang HP. Diffusion-Weighted Imaging of Upper Abdominal Organs Acquired with Multiple B-Value Combinations: Value of Normalization Using Spleen as the Reference Organ. *Korean J Radiol* 2018;19:389-96.
 7. Sandberg JK, Young VA, Syed AB, Yuan J, Hu Y, Sandino C, Menini A, Hargreaves B, Vasanaawala S. Near-Silent and Distortion-Free Diffusion MRI in Pediatric Musculoskeletal Disorders: Comparison With Echo Planar Imaging Diffusion. *J Magn Reson Imaging* 2021;53:504-13.
 8. Chen Y, Yang P, Fu C, Bian Y, Shao C, Ma C, Lu J. Variabilities in apparent diffusion coefficient (ADC) measurements of the spleen and the paraspinal muscle: A single center large cohort study. *Heliyon* 2023;9:e18166.
 9. Padhani AR, van Ree K, Collins DJ, D'Sa S, Makris A. Assessing the relation between bone marrow signal intensity and apparent diffusion coefficient in diffusion-weighted MRI. *AJR Am J Roentgenol* 2013;200:163-70.
 10. Raya JG, Duarte A, Wang N, Mazzoli V, Jaramillo D, Blamire AM, Dietrich O. Applications of Diffusion-Weighted MRI to the Musculoskeletal System. *J Magn Reson Imaging* 2023. [Epub ahead of print]. doi: 10.1002/jmri.28870.
 11. Zbýň Š, Kajabi AW, Nouraei CM, Ludwig KD, Johnson CP, Tompkins MA, Nelson BJ, Zhang L, Moeller S, Marette S, Metzger GJ, Carlson CS, Ellermann JM. Evaluation of lesion and overlying articular cartilage in patients with juvenile osteochondritis dissecans of the knee using quantitative diffusion MRI. *J Orthop Res* 2023;41:1449-63.
 12. Ukai T, Sato M, Yamashita T, Imai Y, Mitani G, Takagaki T, Serigano K, Mochida J. Diffusion tensor imaging can detect the early stages of cartilage damage: a comparison study. *BMC Musculoskelet Disord* 2015;16:35.
 13. Hamaguchi H, Kitagawa M, Sakamoto D, Katscher U, Sudo H, Yamada K, Kudo K, Tha KK. Quantitative Assessment of Intervertebral Disc Composition by MRI: Sensitivity to Diurnal Variation. *Tomography* 2023;9:1029-40.
 14. Shen S, Wang H, Zhang J, Wang F, Liu SR. Diffusion Weighted Imaging, Diffusion Tensor Imaging, and T2* Mapping of Lumbar Intervertebral Disc in Young Healthy Adults. *Iran J Radiol* 2016;13:e30069.
 15. Niu G, Yang J, Wang R, Dang S, Wu EX, Guo Y. MR imaging assessment of lumbar intervertebral disk degeneration and age-related changes: apparent diffusion coefficient versus T2 quantitation. *AJNR Am J Neuroradiol* 2011;32:1617-23.
 16. Niinimäki J, Korkiakoski A, Parviainen O, Haapea M, Kuisma M, Ojala RO, Karppinen J, Korpelainen R, Tervonen O, Nieminen MT. Association of lumbar artery narrowing, degenerative changes in disc and endplate and apparent diffusion in disc on postcontrast enhancement of lumbar intervertebral disc. *MAGMA* 2009;22:101-9.
 17. Byun WM, Jang HW, Kim SW, Jang SH, Ahn SH, Ahn MW. Diffusion-weighted magnetic resonance imaging of sacral insufficiency fractures: comparison with metastases of the sacrum. *Spine (Phila Pa 1976)* 2007;32:E820-4.
 18. Le Bihan D, Turner R, Moonen CT, Pekar J. Imaging of diffusion and microcirculation with gradient sensitization: design, strategy, and significance. *J Magn Reson Imaging* 1991;1:7-28.
 19. Rosenkrantz AB, Oei M, Babb JS, Niver BE, Taouli B. Diffusion-weighted imaging of the abdomen at 3.0 Tesla: image quality and apparent diffusion coefficient reproducibility compared with 1.5 Tesla. *J Magn Reson Imaging* 2011;33:128-35.
 20. Wáng YXJ. Gender-specific liver aging and magnetic resonance imaging. *Quant Imaging Med Surg* 2021;11:2893-904.
 21. Yu WL, Xiao BH, Ma FZ, Zheng CJ, Tang SN, Wáng YXJ. Underestimation of the spleen perfusion fraction by intravoxel incoherent motion MRI. *NMR Biomed* 2023;36:e4987.
 22. Wang YXJ. Complicated relationships between tissue T2 relaxation time and in vivo tissue diffusion measures, depending on the ranges of T2 value. arXiv:2306.10657.
 23. Wáng YXJ, Zhao KX, Ma FZ, Xiao BH. The contribution

- of T2 relaxation time to MRI-derived apparent diffusion coefficient (ADC) quantification and its potential clinical implications. *Quant Imaging Med Surg* 2023;13:7410-6.
24. Wáng YXJ, Ma FZ. A tri-phasic relationship between T2 relaxation time and magnetic resonance imaging (MRI)-derived apparent diffusion coefficient (ADC). *Quant Imaging Med Surg* 2023. doi: 10.21037/qims23-1342.
 25. Wáng YXJ. The very low magnetic resonance imaging apparent diffusion coefficient (ADC) measure of abscess is likely due to pus's specific T2 relaxation time. *Quant Imaging Med Surg* 2023. doi: 10.21037/qims-23-1363.
 26. Wall SD, Fisher MR, Amparo EG, Hricak H, Higgins CB. Magnetic resonance imaging in the evaluation of abscesses. *AJR Am J Roentgenol* 1985;144:1217-21.
 27. de Bazelaire CM, Duhamel GD, Rofsky NM, Alsop DC. MR imaging relaxation times of abdominal and pelvic tissues measured in vivo at 3.0 T: preliminary results. *Radiology* 2004;230:652-9.
 28. Bogaert J, Claessen G, Dresselaers T, Masci PG, Belge C, Delcroix M, Symons R. Magnetic resonance relaxometry of the liver - a new imaging biomarker to assess right heart failure in pulmonary hypertension. *J Heart Lung Transplant* 2022;41:86-94.
 29. Lang P, Wendland MF, Saeed M, Gindele A, Rosenau W, Mathur A, Gooding CA, Genant HK. Osteogenic sarcoma: noninvasive in vivo assessment of tumor necrosis with diffusion-weighted MR imaging. *Radiology* 1998;206:227-35.
 30. Pettersson H, Slone RM, Spanier S, Gillespy T 3rd, Fitzsimmons JR, Scott KN. Musculoskeletal tumors: T1 and T2 relaxation times. *Radiology* 1988;167:783-5.
 31. Gold GE, Han E, Stainsby J, Wright G, Brittain J, Beaulieu C. Musculoskeletal MRI at 3.0 T: relaxation times and image contrast. *AJR Am J Roentgenol* 2004;183:343-51.
 32. Roth C, Hirsch FW, Sorge I, Kiess W, Jurkutat A, Witt M, Böker E, Gräfe D. Preclinical Cartilage Changes of the Knee Joint in Adolescent Competitive Volleyball Players: A Prospective T2 Mapping Study. *Rofo* 2023;195:913-23.
 33. Ruiz Santiago F, Pozuelo Calvo R, Almansa López J, Guzmán Álvarez L, Castellano García MDM. T2 mapping in patellar chondromalacia. *Eur J Radiol* 2014;83:984-8.
 34. Wáng YX, Zhao F, Griffith JF, Mok GS, Leung JC, Ahuja AT, Yuan J. T1rho and T2 relaxation times for lumbar disc degeneration: an in vivo comparative study at 3.0-Tesla MRI. *Eur Radiol* 2013;23:228-34.
 35. Yang L, Sun C, Gong T, Li Q, Chen X, Zhang X. T1ρ, T2 and T2* mapping of lumbar intervertebral disc degeneration: a comparison study. *BMC Musculoskelet Disord* 2022;23:1135.
 36. Stelzeneder D, Welsch GH, Kovács BK, Goed S, Paternostro-Sluga T, Vlychou M, Friedrich K, Mamisch TC, Trattng S. Quantitative T2 evaluation at 3.0T compared to morphological grading of the lumbar intervertebral disc: a standardized evaluation approach in patients with low back pain. *Eur J Radiol* 2012;81:324-30.
 37. Bouhsina N, Tur L, Hardel JB, Madec S, Rouleau D, Etienne F, Guicheux J, Clouet J, Fusellier M. Variable flip angle T1 mapping and multi-echo T2 and T2* mapping magnetic resonance imaging sequences allow quantitative assessment of canine lumbar disc degeneration. *Vet Radiol Ultrasound* 2023;64:864-72.
 38. Arita Y, Takahara T, Yoshida S, Kwee TC, Yajima S, Ishii C, Ishii R, Okuda S, Jinzaki M, Fujii Y. Quantitative Assessment of Bone Metastasis in Prostate Cancer Using Synthetic Magnetic Resonance Imaging. *Invest Radiol* 2019;54:638-44.
 39. Jung Y, Gho SM, Back SN, Ha T, Kang DK, Kim TH. The feasibility of synthetic MRI in breast cancer patients: comparison of T(2) relaxation time with multiecho spin echo T(2) mapping method. *Br J Radiol* 2018;92:20180479.
 40. Baohong W, Jing Z, Zanzia Z, Kun F, Liang L, Eryuan G, Yong Z, Fei H, Jingliang C, Jinxia Z. T2 mapping and readout segmentation of long variable echo-train diffusion-weighted imaging for the differentiation of parotid gland tumors. *Eur J Radiol* 2022;151:110265.
 41. Hepp T, Kalmbach L, Kolb M, Martirosian P, Hilbert T, Thaiss WM, Notohamiprodjo M, Bedke J, Nikolaou K, Stenzl A, Kruck S, Kaufmann S. T2 mapping for the characterization of prostate lesions. *World J Urol* 2022;40:1455-61.
 42. Gu W, Fang S, Hou X, Ma D, Li S. Exploring diagnostic performance of T2 mapping in diffuse glioma grading. *Quant Imaging Med Surg* 2021;11:2943-54.
 43. Oh J, Cha S, Aiken AH, Han ET, Crane JC, Stainsby JA, Wright GA, Dillon WP, Nelson SJ. Quantitative apparent diffusion coefficients and T2 relaxation times in characterizing contrast enhancing brain tumors and regions of peritumoral edema. *J Magn Reson Imaging* 2005;21:701-8.
 44. Bottomley PA, Foster TH, Argersinger RE, Pfeifer LM. A review of normal tissue hydrogen NMR relaxation times and relaxation mechanisms from 1-100 MHz: dependence on tissue type, NMR frequency, temperature, species, excision, and age. *Med Phys* 1984;11:425-48.

45. Greenway CV, Stark RD. Hepatic vascular bed. *Physiol Rev* 1971;51:23-65.
46. Feraco P, Donner D, Gagliardo C, Leonardi I, Piccinini S, Del Poggio A, Franciosi R, Petralia B, van den Hauwe L. Cerebral abscesses imaging: A practical approach. *J Popul Ther Clin Pharmacol* 2020;27:e11-24.
47. Harish S, Chiavaras MM, Kotnis N, Rebello R. MR imaging of skeletal soft tissue infection: utility of diffusion-weighted imaging in detecting abscess formation. *Skeletal Radiol* 2011;40:285-94.
48. Subhawong TK, Durand DJ, Thawait GK, Jacobs MA, Fayad LM. Characterization of soft tissue masses: can quantitative diffusion weighted imaging reliably distinguish cysts from solid masses? *Skeletal Radiol* 2013;42:1583-92.
49. Erdogan C, Hakyemez B, Yildirim N, Parlak M. Brain abscess and cystic brain tumor: discrimination with dynamic susceptibility contrast perfusion-weighted MRI. *J Comput Assist Tomogr* 2005;29:663-7.
50. Morán LM, Vega J, Gómez-León N, Royuela A. Myxomas and myxoid liposarcomas of the extremities: Our preliminary findings in conventional, perfusion, and diffusion magnetic resonance. *Acta Radiol Open* 2022;11:20584601221131481.
51. Einarsdóttir H, Karlsson M, Wejde J, Bauer HC. Diffusion-weighted MRI of soft tissue tumours. *Eur Radiol* 2004;14:959-63.
52. Subhawong TK, Jacobs MA, Fayad LM. Insights into quantitative diffusion-weighted MRI for musculoskeletal tumor imaging. *AJR Am J Roentgenol* 2014;203:560-72.
53. Hayashida Y, Hirai T, Yakushiji T, Katahira K, Shimomura O, Imuta M, Nakaura T, Utsunomiya D, Awai K, Yamashita Y. Evaluation of diffusion-weighted imaging for the differential diagnosis of poorly contrast-enhanced and T2-prolonged bone masses: Initial experience. *J Magn Reson Imaging* 2006;23:377-82.
54. Ahlwat S, Khandheria P, Subhawong TK, Fayad LM. Differentiation of benign and malignant skeletal lesions with quantitative diffusion weighted MRI at 3T. *Eur J Radiol* 2015;84:1091-7.
55. Feuerlein S, Pauls S, Juchems MS, Stuber T, Hoffmann MH, Brambs HJ, Ernst AS. Pitfalls in abdominal diffusion-weighted imaging: how predictive is restricted water diffusion for malignancy. *AJR Am J Roentgenol* 2009;193:1070-6.
56. Balliu E, Vilanova JC, Peláez I, Puig J, Remollo S, Barceló C, Barceló J, Pedraza S. Diagnostic value of apparent diffusion coefficients to differentiate benign from malignant vertebral bone marrow lesions. *Eur J Radiol* 2009;69:560-6.
57. Surov A, Eger KI, Potratz J, Gottschling S, Wienke A, Jechorek D. Apparent diffusion coefficient correlates with different histopathological features in several intrahepatic tumors. *Eur Radiol* 2023;33:5955-64.
58. Thormann M, Surov A, Pech M, March C, Hass P, Damm R, Omari J. Local ablation of hepatocellular carcinoma by interstitial brachytherapy: prediction of outcome by diffusion-weighted imaging. *Acta Radiol* 2023;64:1331-40.
59. Stadnik TW, Chaskis C, Michotte A, Shabana WM, van Rompaey K, Luypaert R, Budinsky L, Jellus V, Osteaux M. Diffusion-weighted MR imaging of intracerebral masses: comparison with conventional MR imaging and histologic findings. *AJNR Am J Neuroradiol* 2001;22:969-76.
60. Sadeghi N, D'Haene N, Decaestecker C, Levivier M, Metens T, Maris C, Wikler D, Baleriaux D, Salmon I, Goldman S. Apparent diffusion coefficient and cerebral blood volume in brain gliomas: relation to tumor cell density and tumor microvessel density based on stereotactic biopsies. *AJNR Am J Neuroradiol* 2008;29:476-82.
61. Rosenkrantz AB, Matza BW, Sabach A, Hajdu CH, Hindman N. Pancreatic cancer: lack of association between apparent diffusion coefficient values and adverse pathological features. *Clin Radiol* 2013;68:e191-7.
62. Nonomura Y, Yasumoto M, Yoshimura R, Haraguchi K, Ito S, Akashi T, Ohashi I. Relationship between bone marrow cellularity and apparent diffusion coefficient. *J Magn Reson Imaging* 2001;13:757-60.
63. Rygh CB, Wang J, Thuen M, Gras Navarro A, Huuse EM, Thorsen F, Poli A, Zimmer J, Haraldseth O, Lie SA, Enger PØ, Chekenya M. Dynamic contrast enhanced MRI detects early response to adoptive NK cellular immunotherapy targeting the NG2 proteoglycan in a rat model of glioblastoma. *PLoS One* 2014;9:e108414.
64. Maeda M, Matsumine A, Kato H, Kusuzaki K, Maier SE, Uchida A, Takeda K. Soft-tissue tumors evaluated by line-scan diffusion-weighted imaging: influence of myxoid matrix on the apparent diffusion coefficient. *J Magn Reson Imaging* 2007;25:1199-204.
65. Razeq A, Nada N, Ghaniem M, Elkhamary S. Assessment of soft tissue tumours of the extremities with diffusion echoplanar MR imaging. *Radiol Med* 2012;117:96-101.
66. Mazaheri Y, Hötter AM, Shukla-Dave A, Akin O, Hricak H. Effect of intravascular contrast agent on diffusion and perfusion fraction coefficients in the peripheral zone and prostate cancer. *Magn Reson Imaging* 2018;51:120-7.
67. Arponen O, Sudah M, Sutela A, Taina M, Masarwah A, Liimatainen T, Vanninen R. Gadoterate meglumine

- decreases ADC values of breast lesions depending on the b value combination. *Sci Rep* 2018;8:87.
68. Maldjian JA, Listerud J, Moonis G, Siddiqi F. Computing diffusion rates in T2-dark hematomas and areas of low T2 signal. *AJNR Am J Neuroradiol* 2001;22:112-8.
 69. Silvera S, Oppenheim C, Touzé E, Ducreux D, Page P, Domigo V, Mas JL, Roux FX, Frédy D, Meder JF. Spontaneous intracerebral hematoma on diffusion-weighted images: influence of T2-shine-through and T2-blackout effects. *AJNR Am J Neuroradiol* 2005;26:236-41.
 70. Xiao BH, Wáng YXJ. Different tissue types display different signal intensities on b = 0 images and the implications of this for intravoxel incoherent motion analysis: Examples from liver MRI. *NMR Biomed* 2021;34:e4522.
 71. Chandarana H, Do RK, Mussi TC, Jensen JH, Hajdu CH, Babb JS, Taouli B. The effect of liver iron deposition on hepatic apparent diffusion coefficient values in cirrhosis. *AJR Am J Roentgenol* 2012;199:803-8.
 72. Kim Y, Lee SK, Kim JY, Kim JH. Pitfalls of Diffusion-Weighted Imaging: Clinical Utility of T2 Shine-through and T2 Black-out for Musculoskeletal Diseases. *Diagnostics (Basel)* 2023;13:1647.
 73. Kinoshita M, Uchikoshi M, Tateishi S, Miyazaki S, Sakai M, Ozaki T, Asai K, Fujita Y, Matsuhashi T, Kanemura Y, Shimosegawa E, Hatazawa J, Nakatsuka SI, Kishima H, Nakanishi K. Magnetic Resonance Relaxometry for Tumor Cell Density Imaging for Glioma: An Exploratory Study via (11)C-Methionine PET and Its Validation via Stereotactic Tissue Sampling. *Cancers (Basel)* 2021;13:4067.
 74. Cieszanowski A, Anysz-Grodzicka A, Szeszkowski W, Kaczynski B, Maj E, Gornicka B, Grodzicki M, Grudzinski IP, Stadnik A, Krawczyk M, Rowinski O. Characterization of focal liver lesions using quantitative techniques: comparison of apparent diffusion coefficient values and T2 relaxation times. *Eur Radiol* 2012;22:2514-24.
 75. Wáng YXJ. Mutual constraining of slow component and fast component measures: some observations in liver IVIM imaging. *Quant Imaging Med Surg* 2021;11:2879-87.
 76. Wáng YXJ. A reduction of perfusion can lead to an artificial elevation of slow diffusion measure: examples in acute brain ischemia MRI intravoxel incoherent motion studies. *Ann Transl Med* 2021;9:895.
 77. Wáng YXJ. Observed paradoxical perfusion fraction elevation in steatotic liver: An example of intravoxel incoherent motion modeling of the perfusion component constrained by the diffusion component. *NMR Biomed* 2021;34:e4488.

Cite this article as: Wáng YXJ, Aparisi Gómez MP, Ruiz Santiago F, Bazzocchi A. The relevance of T2 relaxation time in interpreting MRI apparent diffusion coefficient (ADC) map for musculoskeletal structures. *Quant Imaging Med Surg* 2023;13(12):7657-7666. doi: 10.21037/qims-23-1392